International Journal of Control and Automation
Vol.7, No.8 (2014), pp. 209-220
http://dx.doi.org/10.14257/ijca.2014.7.8.18

Dynamic Testing and Fault Diagnosis of CNC Based on the Method of Cepstrum Identification

Yuhou Wu[1,2, a], Dehong Zhao[1,2, b], Sun Jing[2,c] and Ke Zhang[2,d]

[1]*School of Mechanical Engineering, Dalian University of Technology, Dalian, China*
[2]*College of Traffic & Mechanical Engineering, Shenyang Jianzhu University, Shenyang, China*
[a] *yuhwu@sjzu.edu.cn*, [b]*85755340@qq.com*, [c]*906285149@qq.com*, [d] *764924307@qq.com*

Abstract

Vibration characteristic of mechanical system is the main factor affecting machine tool accuracy and longevity. The HTM50200 CNC with eight axles and double five-axis linkage was tested by a self-made vibration test system. The dynamic characteristic and fault diagnosis was analyzed by using the method of cepstrum identification on the vibration signal of X, Y, Z direction of the principal axis front. Analysis shows that the machining center has good dynamic characteristics, and has no obvious potential problems; the machining center is greatly influenced by Spindle cutter handle system; obtain the optimal processing parameters for machining center.

Keywords: *Dynamic Testing; Fault Diagnosis; Method of Cepstrum Identification*

1. Introduction

Any moving parts will produce vibration. The difference is vibration amplitude, and some vibration can affect the normal work of the structure [1]. From fig.1 we can see that a product before produces larger vibration, has a long working time, but once there is obvious vibration accompanied by a certain noise, its life will decline sharply [2-3]. If the corresponding repair measures are not taken, the product will soon enter the ranks of the damage. So the vibration test to structural elements of the movement is necessary. And for NC machine tool, in order to improve the machining precision of workpiece, avoid causing more serious damage to the machine tool, the vibration test appears especially important [4-5].

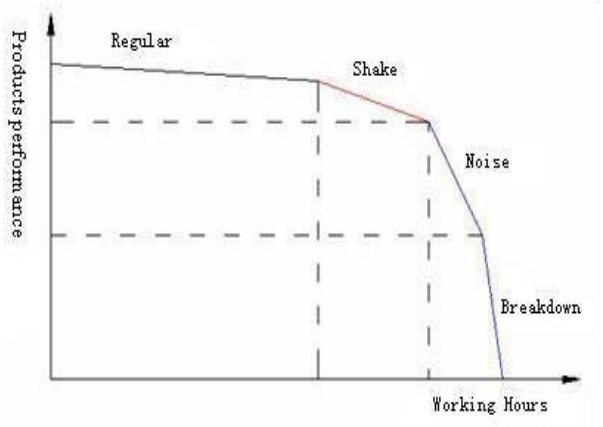

Figure 1. The Relation Curve of Structure Performance

ISSN: 2005-4297 IJCA

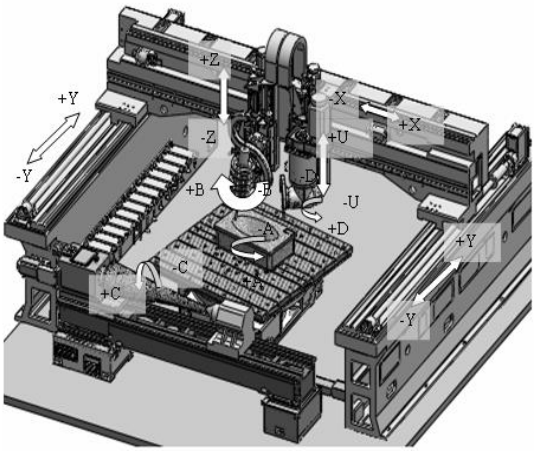

Figure 2. HTM50200 CNC MC Construction

NC machine tool vibration caused by many factors, Comparison of several common vibration conditions are as follows [6]:

(1) Installation problems. Such as the anchor bolt of machine tool become flexible or there is no anchor bolt. When machine tool X, Y axis fast move back and forth, machine tool will vibrate significantly.

(2) The problem of processing program. In order to avoid error when go circular, for example, smaller filter is adopted, but that led to the generated program is very intensive, It will produces vibration phenomenon on a machine tool with bad acceleration.

(3) Electrical components failure problems. For example when the detecting element of encoder closed-loop system makes the feedback signal unstable because of dirt or damage or something wrong with connecting line, the inverter and servo drive parts will constantly adjust the frequency and voltage according to the signal, and are expected to get command speed. That leads to motor constant accelerates and decelerates, and then causes machine vibration.

(4) Several vibration factors above can be classified as forced vibration type. It assumes that the machine or spare parts have similar characteristics with the elastic quality system. When the machine tool has outside force which can change over time, it will produce forced vibration consistent with action frequency. If the vibration frequency has the same inherent frequency with a system of machine tool, it will be vibration or resonance more intense. There is a vibration type called self-excited vibration. For example, chatter phenomenon in the process of cutting is the most typical of self-excited vibration; it is not caused by the external excitation up, but happens when cutting force energy constantly accumulates. About the reason and mechanism of the cutting chatter scholars at home and abroad already have a lot of researches. After analyzing the causes of chatter, F.W.Taylor [7] proposed: It is one of the main causes of flutter that the frequency forming the discontinuous cutting is the same with one of the cutting tool and workpiece or the transmission system of the machine tool. From the start, with in-depth study of flutter mechanism, chatter could be divided into the following several types: R.N.Arnold [8] propose that it is one of the major reasons for flutter that the main component of cutting force produces the self-excited vibration relative to the decline characteristics of the cutting speed. R.S.Hahn [9] thinks that the emergence of machine cutting chatter is formed by the difference of cutting tool cutting thickness caused by phase difference between the last cutting marks and the vibration displacement of the cutting tool ;Tlusty and Koenigsberger [10] think that when the cutting tool and workpiece vibration in two perpendicular directions at the same time will occur flutter, called type coupling flutter; There was hybrid flutter inspired by regeneration effect and outside force incentive.

The HTM50200 CNC (Figure 2), with eight axes and double five-axis linkage, was designed for stone material [11]. It has two working head, one for milling, the other for sawing, and two workbenches. Stone cutting properties is discontinuous, instability and Chatter, needs high-rigidity and hyperstability for mechanical system [12]. In this paper, the dynamic characteristic and fault diagnosis was analyzed by using the method of cepstrum identification on the vibration signal of X, Y, Z direction of the principal axis front.

2. Fault Signal Characteristics

Any running mechanical has vibration. The operation of the machinery needs energy. The force will be produced during energy conversion process, and then some certain vibration will be aroused directly or indirectly [13]. As long as the machine runs steady, or its operation changes only within certain limits, the mechanical vibration will be stable. And when the machine is in good condition, the vibration frequency spectrum has certain characteristics. When mechanical failure occurs, there will be important changes in the running state, and the amount of vibration and vibration spectrum will change obviously. Here, with emphasis on the rotating machinery is introduced.

2.1. Failure Characteristics of Shaft and Shaft System

The fault signal of shaft and the shaft system generated by the rotation movement is caused by imbalance, and the axial deformation caused by the wrong. Analysis respectively as follows [14]:

(1) The imbalance the imbalance of shaft generated an unbalanced moment, in the options. That provoked a periodic vibration, the vibration frequency is $f0$=n/60(Hz), n is the shaft speed: $f0$ is a first-order transfer frequency of shaft system.

(2) Shafting installation is not correct Bad shafting installation, shaft bending and the interstice of related parts of the shaft will cause shafting can't very good on the middle, that will causes vibration in the operation. Two shaft axes are paralleled but not overlapping. Both two phases cross axes and two axes space crisscross are on the bad. Misalignment will provoke the axial vibration. Its frequency as opposed to a first-order transfer frequency $f0$; Misalignment will provoke transverse vibration at the same time. Sometimes, the harmonic components are complex. But it often shows as the second order frequency vibration. Sometimes in addition to second order harmonic frequency, it also has apparent first order and third order and high order harmonic frequency vibration.

(3) The bending of shaft the bending of shaft is usually caused by poor self-respect or install, its essence likes misalignment. This fault can also cause the vibration of axial turn first order frequency and horizontal first order and second order frequency.

(4) Fixed edge is loose Solid joint looseness is often caused by the above several kinds of fault vibration. Solid joint looseness arouses fault vibration signals, its frequency is (0.3~0.5) $f0$、 $f0$and higher order vibration frequency.

2.2. The Fault Signal Characteristics of Rolling Bearing

Figure 3 is a geometrical relationship of radial roller bearing. Suppose every contact element bearings are rigid. They are still maintaining their precise geometry under the action of load. And they are only rolling in the movement. For the radial roller bearing in Figure 1, its inner ring is fixed on the shaft and shaft rotate together, and the outer ring is fixed. The distance from rolling contact points A, B and rolling centers o1 to the center of the rotating shaft are (D-dcosa)/2, (D+dcosa)/2 and D/2. Several rotation frequency and blade passing frequency can be obtained. Now as follows derived, respectively [15]:

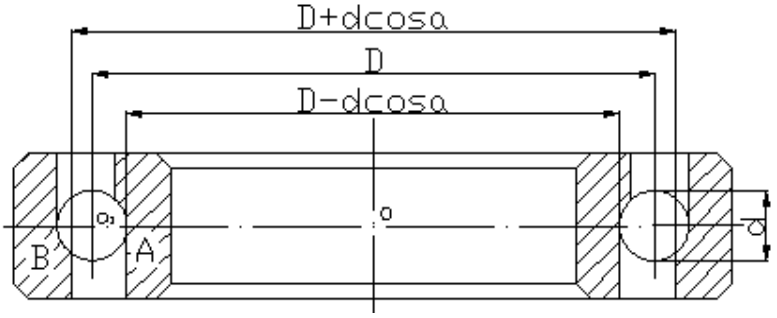

Figure 3. The Structure Schematic Drawing of Rolling Bearing

The frequency of inner ring rotation Due to the rotation together of inner ring and the axis, the speed of the shaft n is transformed into Hz. That is:

$$f_0 = N/60 \tag{1}$$

Keeping the rotation frequency of frame with the cage revolving around axis o, ball bearing makes around, too. Ball in the race makes pure roll. The speed of contact A is equal to the inner ring. That is:

$$V_A = [2\pi 2\pi - dcosa)/2]f_0 = (D - dcosa)\ \pi c_0 \tag{2}$$

Due to the fixed outer ring, point B is the instantaneous center of velocity of a ball. The speed of the ball bearing centers should be expressed as:

$$V_{o1} = \frac{1}{2}V_A = \frac{\pi}{2}f_0(D - dcosa) \tag{3}$$

The frequency of revolution that the ball bearing revolved around axis o can be expressed as:

$$f_o = \frac{V_{o1}}{\pi D} = \frac{1}{2}f_0(1 - \frac{d}{D}cosa) \tag{4}$$

f_o is the rotation frequency of cage.

Ball's rotation frequency The relationship between ball's rotation movement and cage's movement is that they reverse rotation around the o1and o, respectively. The ratio of the rotation frequency can be expressed as:

$$\frac{f_b}{f_o} = \frac{oB}{o_1B} = \frac{(D + dcosa)/2}{(dcosa)/2} = \frac{D}{dcosa}(1 - \frac{dcosa}{D}) \tag{5}$$

Then ball's rotation frequency can be expressed as:

$$f_b = \frac{D}{dcosa}(1 + \frac{dcosa}{D})f_o = \frac{D}{2dcosa}[1 - (\frac{dcosa}{D})^2]f_0 \tag{6}$$

The frequency of cage through the inner ring can be expressed as:

$$f_{oi} = f_0 - f_o = f_0 - \frac{f_0}{2}(1 - \frac{d}{D}cosa) = \frac{f_0}{2}(1 + \frac{d}{D}cosa) \tag{7}$$

The frequency of the ball through the inner ring is equal that the number of ball z multiplies by rotational frequency of the cage:

$$f_{bi} = zf_{oi} = \frac{z}{2}(1 + \frac{d}{D}\cos a) \quad f_0 \tag{8}$$

The ball through the outer frequency the outer ring is fixed, so the frequency is equal that z multiplies by the rotational frequency of the cage fo:

$$f_{be} = zf_{o} = \frac{z}{2}(1 - \frac{d}{D}\cos a) f_0 \tag{9}$$

After understanding the above-mentioned frequency, it will contributes to the fault diagnosis of bearing. If there is a fault inner ring raceway, such as inner ring peeling, dent, unbalance, *etc.*, $f$bi should be found in the vibration signal; If there is a fault outer ring raceway, such as outer peel, dent, not in the middle, etc. Vibration frequency signal should be found; Ball has a fault, such as steel ball peeling off. When rotating once, it will be on inner and outer ring once. So the failure frequency can be expressed as:

$$f_B = 2f_b = \frac{D}{d\cos a}[1 - (\frac{d\cos a}{D})^2]f_0 \tag{10}$$

According to the spindle design parameters of HTM50200 machining center, we can calculate the fault fundamental frequency of engraving head front bearing, the results shown in the following Table 1:

Table 1. The Fault Frequency of the Front Bearing at different Rotating Speed

rotate speed n	f_0	f_{oi}	f_{bi}	f_{be}	f_B
6000	100	59.66	1312.52	887.48	498.28
8000	133	79.35	1745.7	1180.35	662.71

3. Vibration Test System

3.1. Self-made Vibration Test System

The Vibration part includes signal generator, power amplifier and vibrator. Hammer exciting force used in this study is shown in Figure 4, with a power amplifier further enlarge weaker signal, can promote vibrator. The sensor of piezoelectric acceleration sensor, as shown in Figure 5, was used, because of its small quality, the quality that attached to the structure is smaller, the impact on the test results can be ignored; When doing vibration analysis, if you want a expressed in velocity or displacement data, the acceleration signal integration can be implemented through the built-in integration circuit; Finally if its ability to high frequency noise is higher than the velocity or displacement sensor, we can get more accurate results while doing high frequency analysis[16].

Figure 4. The LC301 Type Shocks Hammer

Figure 5. The ICP Type Acceleration Sensors

The signal and collection system that this test uses is the eight channel 24 INV3018C acquisition of vibration and noise analyzer provided by Beijing Oriental institute; Data processing system uses DASP - V10 engineering software version of the platform. It not only can collect vibration signal in time domain, and doing the probability density and correlation analysis, but also can do Fourier transform, the frequency response function, and coherence analysis and so on in frequency domain. At the same time it can also compose random and sine digital signal source needed for the test. The instrument configuration in vibration test system is shown in Figure 6:

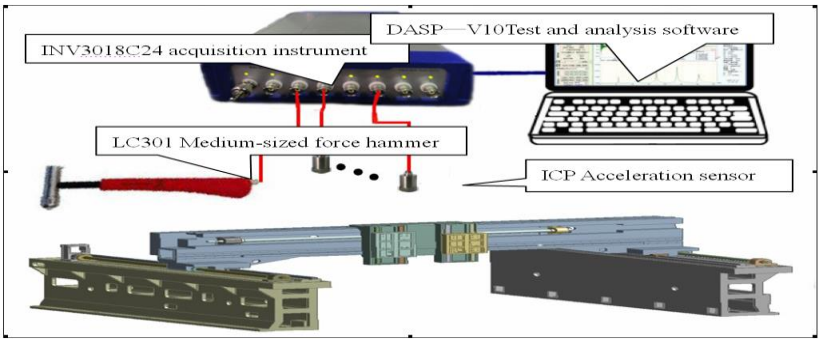

Figure 6. The Structure Schematic Drawing of Vibration Test System

3.2. Testing Scheme and Equipment

Use the center line of the electric main shaft for Z axis, and away from the direction of the vertical table for Z axis forward direction (up); Use With the direction that vertical Z axis and points in column of linear guide for Y axis, back to the operator is the direction of the Y axis forward direction; According to the right-hand rule to determine X. Arrange INV9822 type one-way sensor at the front end bearing spindle, each direction is placed a sensor, a total of three road signs. Specific data acquisition instrument and sensor installation as shown in Figure 7 and Figure 8:

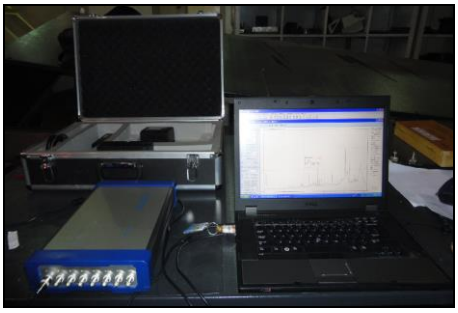

Figure 7. The Instrument Layout on Field Test

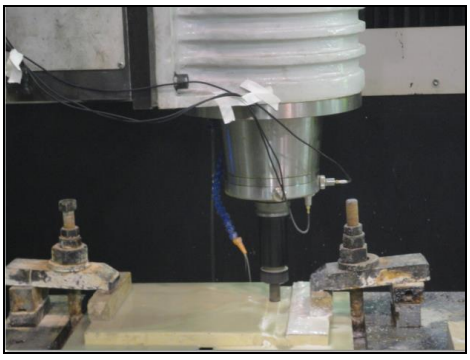

Figure 8. The Arrangement of Sensor

4. Dynamic Test and Analysis of HTM50200 CNC

4.1. Empty Running Test Analysis

Machine idle running test has nothing to do with machining. It evaluates the stationary of machine tools work through idling vibration conditions of the motorized spindle under different rotational speed, and provides data comparison for cutting test analysis. At the same time vibration type that machine tools can produce can be determined, the maximum vibration source can be found out or the extent of potential faults in mechanical structure can be predicted.

Put the vertical milling cutter used in the coarse milling conditions together with the handle on the front end of the motorized spindle, and set its rotating speed respectively 6000 r/min and 8000 r/min speed as the main research. After continuous running half an hour later (Reduce the thermal effect error), pick up the spectral curve of three directions of the machine tool spindle front, when the machine tool operates stability.

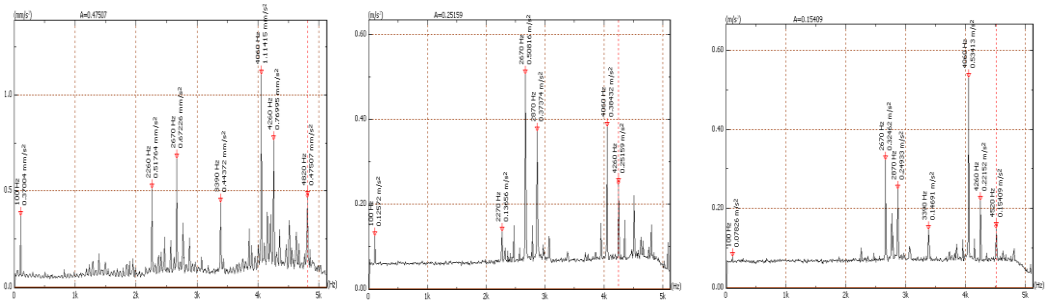

（a） X axis （B） Y axis （C） Z axis

Figure 9. Auto-spectrum of axis (n=6000r/min)

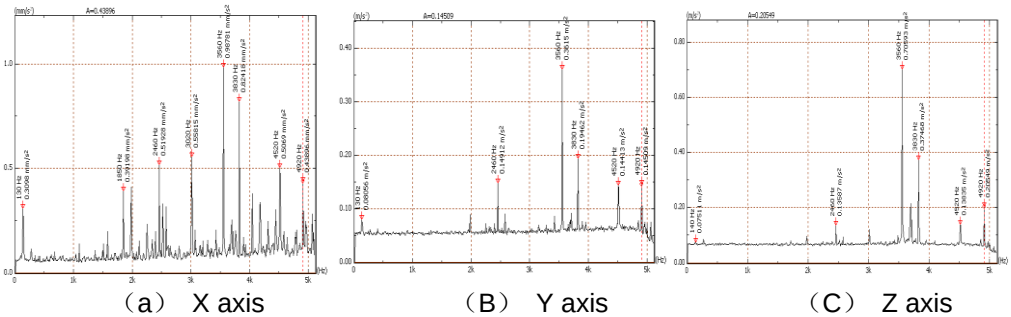

（a） X axis （B） Y axis （C） Z axis

Figure 10. Auto-spectrum of axis (n=8000r/min)

As shown in Figure 9, before 2000 Hz, the vibration amplitude of the spindle was small and waveform change is not big, but bigger peaks appear at 100 Hz. This is caused by spindle imbalance, and the X direction (radial vibration) is most obvious. In addition, we have already calculated spindle front bearing fault fundamental frequency, they are all less than 1500 Hz. This can also be learned thatrolling bearing is in good working order, and have no obvious fault features. Between 2200 Hz and 4500 Hz, there are different degrees of vibration at the three direction of spindle. The X direction has a maximum of 1.12m/s2 at 4060 Hz. Y direction has a maximum of 0.51m/s2 at 2670 Hz. Z direction has a maximum of 0.53m/s2 at 4060Hz.

As shown in Figure 10, the vibration condition of spindle is similar to the previous speed spindle, but the vibration amplitude decreases throughout the analysis frequency, the maximum peak point change. For example the X direction has a maximum of 0.98m/s2 at 3560 Hz, and both sides appear larger peak point intervals of about 540 Hz, the frequency is three times as much as the rotation of the fundamental frequency fo. This is probably caused by the trace of the spindle or the without load misalignment. At the same time, Y, Z have maximum at 3560 Hz, they are 0.36m/s2 and 0.7m/s2.

4.2. Cutting Test Analysis

(1) Speed n = 6000 r/min, feed rate f = 800 mm/min, the cutting depth ap = 1.5 mm

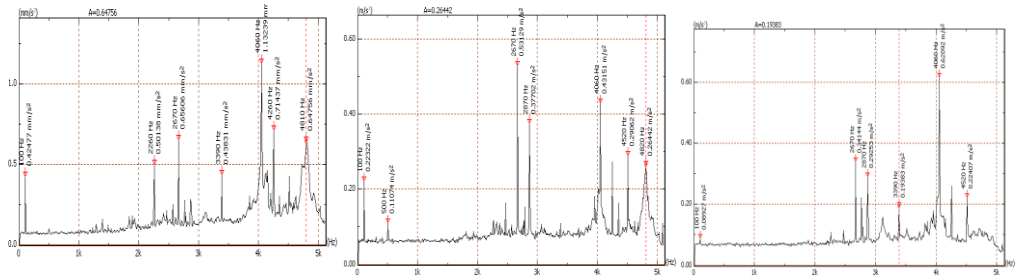

（a） X axis （B） Y axis （C） Z axis

Figure 11. Auto-spectrum of axis (a_p=1.5mm, n=6000r/min, f = 800 mm/min)

As shown in Figure 11, the idling vibration condition of the speed, the peak point of the frequency values have no obvious change, in addition to the amplitude that increased slightly. It can be concluded that it belongs to the stable cutting under the cutting parameters. But the spectrum curve of the Y direction can be seen that the unbalance spindle rotating increased obviously in this direction.

(2) Speed n = 6000 r/min, feed rate f = 800 mm/min, the cutting depth ap = 3mm

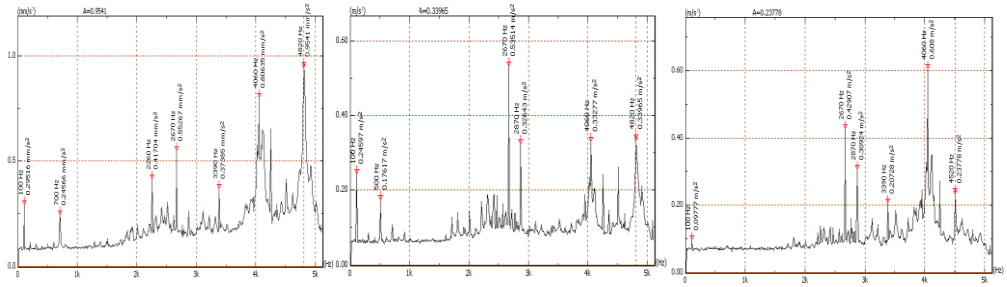

（a） X axis （B） Y axis （C） Z axis

Figure 12. Auto-spectrum of axis (a_p=3mm, n=6000r/min, f = 800 mm/min)

As shown in Figure 12, the cutting depth increased one times, vibration dramatic changes did not occur. It also belongs to the stable cutting process. The maximum peaks

of X direction move from 4060 Hz to 4820 Hz, the vibration amplitude is 0.95m/s2. Y direction has a maximum of 0.54m/s2 at 2670 Hz, Z direction has a maximum of 0.61m/s2 at 4060 Hz.

(3) Speed n = 6000 r/min, feed rate f = 800 mm/min, the cutting depth ap = 4mm

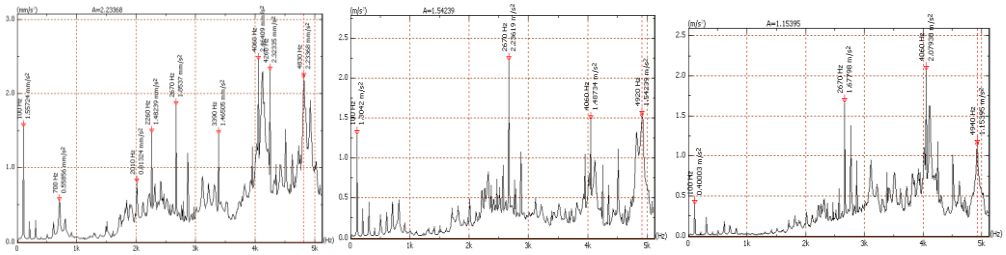

（a） X axis （B） Y axis （C） Z axis

Figure 13. Auto-spectrum of axis (a_p=4mm, n=6000r/min, f = 800 mm/min)

As shown in Figure 13, the vibration condition changes sharply under this cutting parameter, the three direction of the spindle appear interval peaks in low frequency band, interval of frequency is the first order frequency, this suggests that the spindle imbalance and bending features have been reflected in the spectrum curve, and the vibration quantity is bigger. The machining accuracy of machine tools has been influenced seriously. X direction is more scattered at high frequencies of larger peak point distribution, Y, Z direction are mainly concentrated in the vicinity of 2670 Hz,4060 Hz and 4940 Hz, the other frequency bands have smaller amplitude spectrum.. X direction has a maximum of 2.46m/s2 at 4060Hz, Y direction has a maximum of 2.23m/s2 at 2671Hz, Z direction has a maximum of 2.08m/s2 at 4060Hz. Compared with the previous cutting parameters, cutting depth increases 1 mm, the vibration of the spindle increases 3 ~ 4 times. From cutting noise and the surface quality of workpiece, it can be seen that the process as part of the cutting is not smooth.

(4) Speed n = 6000 r/min, feed rate f = 1000 mm/min, the cutting depth ap = 4mm

As shown in Figure 14, in order to further study not smooth cutting, we should control the cutting depth under 4 mm, control the feed rate under 1000 r/min, keep the spindle speed, and feel cutting stability is more unstable than before a parameters from the cutting noise, the phenomenon with smoke happens on the knife. From the spectrum curve of main three directions we can also learn that, in addition to vibration amplitude increases one or two times, the largest peak point near to 2670 Hz and 4060 Hz, and the other frequency amplitude is small. The type is very similar with regeneration chatter features, when cutting chatter occurs, the vibration of main spindle - cutting tool system will be embodied in a frequency point [11]. Judging from this, the cutting process under this cutting parameter belongs to chatter cutting, but flutter body is not necessarily the main shaft.

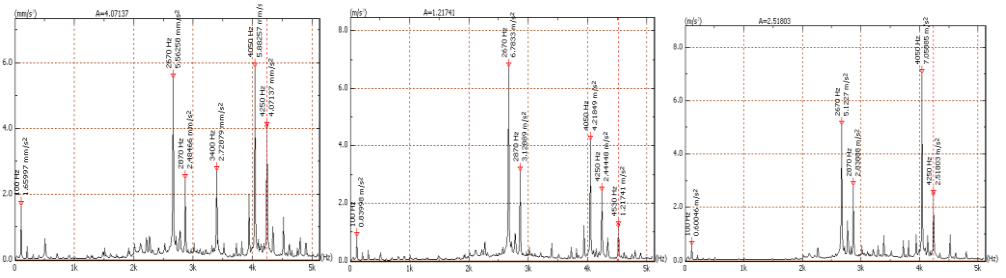

（a） X axis （B） Y axis （C） Z axis

Figure 14. Auto-spectrum of axis (a_p=4mm, n=6000r/min, f = 1000 mm/min)

(5) Speed n = 8000 r/min, feed rate f = 800 mm/min, the cutting depth ap = 1.5mm

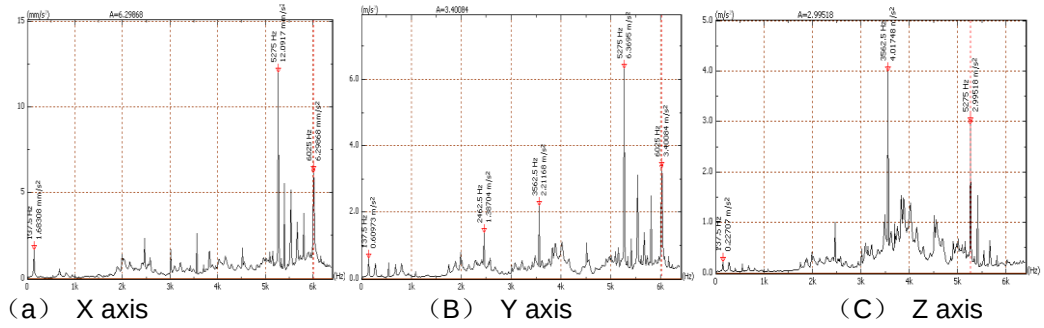

（a） X axis （B） Y axis （C） Z axis

Figure 15. Auto-spectrum of axis (a_p=1.5mm, n=8000r/min, f = 800 mm/min)

As shown in Figure 15, when the spindle speed is 8000 r/min, the feed rate decreases to 800 mm/min. When the cutting depth back to 1.5 mm, compared with 6000 r/min, the low frequency vibration amplitude increases 5 times or so, the biggest increase of high frequency is nearly 10 times, and peak point is relatively concentrated. This is similar to the vibration circumstances of Figure 1.6, there are trace amounts of flutter occur. Compared with the vibration of the cutting parameters before, the large amplitude 12.1 m/s2 is two times the size of which when the cutting depth is 4 mm, except the peaks occur frequency shift.

Figure 16. Work-piece and Cutting Tool after Cutting Test

5. The Test Results Analysis

Combining with the vibration condition of machine idle running and cutting conditions, in rough milling conditions, selecting spindle speed 6000 r/min or so is the most appropriate, cutting depth is controlled within 3 mm, the feed rate does not exceed 1000 mm/min. When choosing the spindle speed 8000 r/min, even cutting depth is small, the vibration is more intense than which under the limit of the cutting parameters when the specific speed is 6000 r/min. When the cutting depth increases slightly, it will produce larger vibration noise, white smoke also occurs on cutting tool, it closes to flutter phenomenon. Figure 16 are the processing traces of the stone sample and the wear condition of the tool after test processing, under different cutting parameters above. In the figure the gold-plated corundum of four milling cutter have been worn away under the extreme working conditions, template has appeared severe burn marks.

6. Conclusion

(1) Through the observation of the low-frequency stage in the spectrum curve of spindle, especially first turn frequency, the vibration peak increase, with the increase of spindle speed. It state that the spindle have trace amounts of bending or misalignment, but the operation performance of rolling bearing is good, there is no obvious potential fault features.

(2) Through doing the spectrum curve analysis to the vibration signals, the best cutting parameters under rough milling conditions have been obtained: the most appropriate spindle speed is around 6000 r/min; cutting depth controlled within 3 mm, the feed rate does not exceed 1000 mm/min

(3) Do the analysis of vibration signal which have different rotational speed, different cutting depth, and different feed rate. Maximum vibration peak point of spindle under the limit cutting parameters concentrate on 2670 Hz and 4060 Hz. Combining with the theory of flutter analysis, we can bring out that these two points are likely to be frequency of cutting chatter, but the subject of flutter is not necessarily the main shaft, probably is the cutting tool shank with system.

Acknowledgements

This work was financially supported by the Innovation Program of Education Commission supported plan (IRT1160), the Liaoning technology Research plan (2011220012), Shenyang Municipal technology Research plan (F12-036-2-00), the Research Project of Liaoning Department of Education (L2011094) and Shenyang Jianzhu University Key Laboratory Foundation (JX-200906).

References

[1] M. Pellegrini, H. Endo, E. Merzari and H. Ninokata, "Algebraic turbulent heat flux model for prediction of thermal stratification in piping systems", Nuclear Technology, vol. 181, no. 1, **(2013)** January, pp. 144-156.
[2] P. Borghesani, P. Pennacchi, R. B. Randall, N. Sawalhi and R. Ricci, "Application of cepstrum pre-whitening for the diagnosis of bearing faults under variable speed conditions", Mechanical Systems and Signal Processing, vol. 36, no. 2, **(2013)** April, pp. 370-384.
[3] G. De Robek, B. Peeters and W. X. Ren, "Benchmark study on system identification through ambient vibration measurements", Proceedings of IMAC 18, the International Modal Analysis Conference, Texas, USA, **(2000)** February.
[4] T, Kijeswski and A. Kareem "Wavelet Transform for System Identification in Civil Engineering", Computer Aided Civil and Infrastructure Engineering, no. 18, **(2003)**, pp. 339-355.
[5] A. H. Chen and J. Zhong, "Description and Prediction of Catastrophe of Vibration State for Faulty Rotors", Trans, NFSOC, vol. 6, no.1, **(2006)**, pp. 130-134.
[6] G.-M. Xian, "Mechanical failure classification for spherical roller bearing of hydraulic injection molding machine using DWT–SVM", Expert Systems with Applications, no. 37, **(2010)**, pp. 6742–6747.
[7] J. Xiao, J. Xu, Z. Chen, K. Zhang and L. Pan, "A hybrid quantum chaotic swarm evolutionary algorithm for DNA encoding", Computers & Mathematics with Applications, no. 57, **(2009)**, pp. 1949-1958.
[8] R. Katz and Y. Koren, "Reconfigurable Machines", ESDA, vol. 59, no. 56, **(2008)**, pp. 145-152.
[9] T.-K. Wu, S.-C. Huang and Y. –R. Meng, "Evaluation of ANN and SVM classifiers as predictors to the diagnosis of students with learning disabilities", Expert Systems with Applications, no. 34, **(2008)**, pp. 1846–1856.
[10] C.-H. Wu, G.-H. Tzeng and R.-H. Lin, "A novel hybrid genetic algorithm for kernel function and parameter optimization in support vector regression", Expert Systems with Applications, no. 36, **(2009)**, pp. 4725–4735.
[11] K. Zhang, D. Zhao and Y. Wu, "The Detection and Analysis of Straightness Errors on Pillar and Guide Rail of Alien Stone Turning-milling Compound Machining Center", Applied Mechanics and Materials, vol. 9, no. 8, **(2011)**, pp. 80-81.
[12] W. Yuhou, Z. Jipeng, L. Songhua and Z. Ke, "Experimental Research on Surface Quality of Si3N4 Ceramic Internal Grinding", Journal of Shenyang Jianzhu University(Natural Science), vol. 01, **(2010)**, pp. 39-42.

[13] W. Yuhou, W. Kai, J. Qingkai and L. Yuedi, "Orthogonal Experiment Research on Specific Grinding Energy of Granite Internal Grinding. Journal of Shenyang Jianzhu University", (Natural Science), vol. 3, **(2009)**, pp. 53-57.
[14] H. Endo, R. B. Randall and C. Gosselin, "Differential diagnosis of spall versus cracks in the gear tooth fillet region", Journal of Failure Analysis and Prevention, vol. 4, no. 5, **(2004)** October, pp. 63-71.
[15] V. Purushotham, S. Narayanan, Prasad and A. N. Suryanarayana, "Multi-fault diagnosis of rolling bearing elements using wavelet analysis and hidden Markov model based fault recognition", NDT and E International, vol. 38, no. 8, **(2005)** December, pp. 654-664.
[16] H. Endo, R. B. Randall and C. Gosselin, "The effects of localized gear tooth damage on the gear dynamics - A comparison of the effect of a gear tooth root crack and a spall on the gear transmission error", IMechE Event Publications, Eighth International Conference on Vibrations in Rotating Machinery - IMechE Conference Transactions, vol. 2004, no. 2, **(2004)** , pp. 333-342.

